Potential Applications of Additive Manufacturing in Intervertebral Disc Replacement Using Gyroid Structures with Various TPU Filaments

Leandro Hippel , Jan Mussler , Dirk Velten , Bernd Rolauffs , Hagen Schmal , Michael Seidenstuecker *

Posted Date: 10 December 2025

doi: 10.20944/preprints202512.0888.v1

Keywords: additive manufacturing; 3D-printing; fused deposition modeling FDM; Gyroid; Intervertebral disc; mechanical properties

Article

Potential Applications of Additive Manufacturing in Intervertebral Disc Replacement Using Gyroid Structures with Various TPU Filaments

Leandro Hippel [1,2], Jan Mussler [1,2], Dirk Velten [2], Bernd Rolauffs [1], Hagen Schmal [3,4] and Michael Seidenstuecker [1,3,*]

[1] G.E.R.N. Tissue Replacement, Regeneration & Neogenesis, Department of Orthopedics and Trauma Surgery, Medical Center-Albert-Ludwigs-University of Freiburg, Faculty of Medicine, Albert-Ludwigs-University of Freiburg, Hugstetter Straße 55, 79106 Freiburg, Germany

[2] Applied Biomechanics, Offenburg University, Badstraße 24, 77652 Offenburg, Germany

[3] Department of Orthopedics and Trauma Surgery, Medical Center-Albert-Ludwigs-University of Freiburg, Faculty of Medicine, Albert-Ludwigs-University of Freiburg, Hugstetter Straße 55, 79106 Freiburg, Germany

[4] Department of Orthopedic Surgery and Traumatology, Odense University Hospital, 5000 Odense, Denmark

* Correspondence: michael.seidenstuecker@uniklinik-freiburg.de

Abstract

Background Disc degeneration is an increasingly common problem in modern society and is often a precursor to a herniated disc. Contributing factors include physical exertion, overuse, the natural aging process, and disease and injury. Over time, the fibrous ring of the disc develops cracks and small tears, allowing fluid from the nucleus pulposum to escape. As a result, the ability of the disc to absorb shock decreases, potentially leading to a bulging or herniated disc. In this work, previously initiated investigations are extended, and additional thermoplastic polyurethane (TPU) filaments are examined with respect to their suitability for additive manufacturing as potential disc replacement materials. **Materials & Methods** To remain comparable, the additive manufacturing in this work is also carried out with Fused Deposition Modeling (FDM) 3D printers and as a Ø50 mm x 10mm disc. The Gyroid was varied from 10 mm^3 for the coarsest structure to 4 mm^3 for the finest structure. The wall thickness of the Gyroid was also varied from 0.5 to 1.0 mm, as were the outer walls of the disc, whose wall thickness was varied from 0.4 to 0.8 mm. Four different TPU filaments (Extrudr FlexSemiSoft, GEEETECH TPU, SUNLU TPU and OVERTURE TPU) were used. This resulted in 36 different settings per filament. The 3D printed discs were analyzed using an Olympus SZ61 stereomicroscope. A tensile test according to DIN EN ISO 527-1 was performed on the 3D printed samples 5A. The aim was to investigate the difference between the different TPU filaments. To test the mechanical properties of the 3D printed discs, a uniaxial compression test was performed with at least three samples of each setting. The body was compressed to 50% of its total height and the force required was recorded as a force-deformation curve. To be comparable to a previous project, a maximum force of 4000–7500 N was used. **Results** Of the 36 different discs tested for each filament, only a maximum of three were within the target range of maximum force. Microscopy revealed that all wall thicknesses were within the target range with only minor variations. The tensile strengths of Geetech, SunLu, and SemiSoft were not significantly different and were in a similar range of 10-11 MPa, with Overture deviating significantly at 9 MPa. The tensile moduli exhibited a comparable distribution: 25-30 MPa for Geetech, SunLu, and SemiSoft, and 17.5 MPa for Overture. **Conclusion** For all of the filaments tested, it was possible to additively produce suitable discs that were within the specified range of 4000-7500 N at 50% compression. This would ensure that these discs would withstand the stresses they would be subjected to in a potential human disc replacement application. Thus, we were able to confirm the suitability of these four filaments, as well as the Gyroid structures, for use as a disc replacement.

 doi:10.20944/preprints202512.0888.v1

Keywords: additive manufacturing; 3D-printing; fused deposition modeling FDM; Gyroid; Intervertebral disc; mechanical properties

1. Introduction

Disc degeneration is an increasingly common problem in modern society and often precedes disc protrusion. Causal factors include physical exertion, overuse, the natural aging process, diseases, and injuries. Over time, the fibrous ring of the intervertebral disc develops cracks and small tears, allowing fluid to escape from the gel-like core. This reduces the disc's ability to absorb shock, which can lead to protrusion or a herniated disc [1]. If conservative treatments are no longer effective, surgical intervention is necessary. The two most important procedures are spinal fusion (spondylodesis), considered the gold standard for treating disc degeneration in the cervical and lumbar spine [1–3]. However, spinal fusion has disadvantages, including limited spinal mobility and increased stress on adjacent vertebral segments. This can accelerate the degeneration of adjacent intervertebral discs, a condition known as adjacent segment degeneration (ASD). ASD leads to pain and nerve compression in the affected region [1,2,4–6]. A new alternative to spinal fusion is the use of artificial disc prostheses. These prostheses are designed to preserve the spine's natural range of motion (ROM) while reducing the risk of ASD [7–10]. According to the Federal Statistical Office, spinal fusion and artificial disc implant procedures will increase in Germany between 2020 and 2022 [11]. The number of spinal fusion procedures is expected to increase by over 2,000, rising from 67,380 in 2020 to 69,728 in 2021. In contrast, the number of artificial disc implantations will remain significantly lower: 4,415 in 2020, 4,205 in 2021, and 3,978 in 2022. From a biomechanical perspective, the human intervertebral disc must be examined in terms of the annulus fibrosus and the nucleus pulposus because it is not a homogeneous material. Cloyd et al. [12] report E-moduli of 0.1–0.5 MPa for the nucleus pulposus and 4–8 MPa for the annulus fibrosus. In contrast, artificial disc prostheses have an elastic modulus of 100–200 GPa due to their metallic titanium components and polymer components such as polyurethane or polyethylene, which have an elastic modulus between 0.5 and 3 GPa [13]. Therefore, they have no shock-absorbing properties. Since 2010, additive manufacturing has been used more and more for medical applications. It can be used to make very precise, custom-made disc prostheses [14]. Various polymeric materials have been explored for this purpose, including flexible polylactic acid (FPLA), which allows for tunable, biomimetic mechanical properties suitable for intervertebral disc tissue engineering [15,16]. These FPLA scaffolds have demonstrated enhanced viscoelasticity and mechanical compatibility with native disc tissue in vitro and in vivo. Similarly, ultra-high molecular weight polyethylene (UHMWPE) has been investigated as a durable structural component for artificial disc replacements, offering favorable wear resistance and improved tensile strength when reinforced with fibers [17]. Such materials demonstrate the potential of polymer-based solutions to bridge the gap between mechanical stability and physiological compliance in intervertebral disc prosthetics. Moreover, the continuous development of additive manufacturing materials expands the range of processable polymers, some of which are now approved for medical use [18]. A previous study [19] investigated whether flexible thermoplastic polyurethane (TPU) filaments could be used to fabricate flexible spinal disc replacements. While that work identified TPU as a highly promising candidate material due to its shock-absorbing properties, the range of printable filaments was limited. In particular, several TPU filaments could not be processed successfully because a drying unit and optimized process parameters were not available at that time. In the present study, this limitation is directly addressed. By implementing an optimized drying protocol at 55 °C before and during printing, along with improved parameter control, it was possible to reliably process those TPU filaments that had previously been unprintable. As a result, the material spectrum investigated here is broader and more representative, allowing for a systematic evaluation of different gyroid geometries and wall designs. Consequently, an extended analysis of additively manufactured TPU gyroid structures with shock-absorbing properties is conducted for their potential application in intervertebral disc replacement. To ensure comparability with the earlier

 doi:10.20944/preprints202512.0888.v1

work [19], standardized Ø50×10mm intervertebral disc specimens are again fabricated using fused deposition modeling (FDM). Consequently, this study can be regarded as a follow-up to the previous study by Gross et al. [19].

2. Materials and Methods

2.1. Materials

For this study, five different flexible TPU filaments were selected: FlexMed and FlexSemiSoft (extrudr, Lustenau, Austria), SUNLU TPU 95A (SUNLU, Zhuhai, China), OVERTURE TPU (Overture 3D Technologies LLC, Houston, USA), and GEEETECH TPU (HK GETECH Co., Shenzhen, China). To clearly differentiate them during handling, the filaments were used in distinct colors: FlexSemiSoft (transparent), SUNLU (orange), OVERTURE (purple), and GEEETECH (light brown, semi-transparent). An overview of their physical and mechanical properties is given in Table 1.

Table 1. Comparison of the mechanical and physical properties of TPU filaments (manufacturer's specifications).

Filament	Shore A	Density [g/cm³]	Tensile Strength [MPa]*	Elongation at break [%]**	Tg [°C]	Tm [°C]
SUNLU	95	1.23	21.7	536	-24	190-220
OVERTURE	95	1.18	30.1	332	-23	210
GEEETECH	95	1.30	23.6	525	-24	185-220
SemiSoft	85	1.18	42	550	-24	180-230

* ISO 527-2; **ASTM D638

2.2. Methods

2.2.1. Filament Preparation

Before processing, all filaments were conditioned to reduce moisture uptake. Drying was performed in a Creality Space Pi Drying Box (Creality 3D Technology Co., Ltd., Shenzhen, China) at 55 °C for at least five hours. The dried filament was then directly guided via a 2 mm PTFE tube from the drying chamber to the extruder, preventing reabsorption of humidity during printing. Two different printers were used for fabrication: a Prusa MK3S+ (Prusa Research, Prague, Czech Republic) and a Sovol SV04 (Sovol, Shenzhen, China). Throughout the printing process, the spools remained inside the heated drying chamber.

2.2.2. 3D Printing Parameter Optimization

To establish suitable process parameters, temperature towers were produced for each filament type to identify the best printing temperature and extrusion speed. Representative examples for FlexSemiSoft, SUNLU, GEEETECH, and OVERTURE are shown in Figure 1. The trials demonstrated that variations in temperature strongly influence surface quality, ranging from stringing effects to incomplete structures. Based on these results, optimized parameter settings were determined. The final values applied in the experiments are highlighted in bold and blue in Table 2.

 doi:10.20944/preprints202512.0888.v1

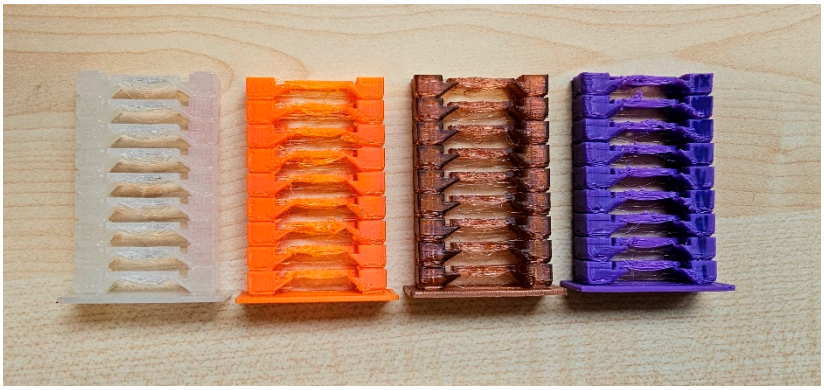

Figure 1. Exemplary illustration of temperature towers made of SemiSoft (transparent), SUNLU (orange), GEEETECH (brown) and OVERTURE (purple) TPU filaments. Temperatures were varied in each step. Printing errors such as stringing are clearly visible at different temperature settings.

Table 2. Temperatures of the different levels of the temperature tower for the TPU filaments used. Arrangement of levels as shown in Figure 1. Final temperatures used for 3D printing are shown in blue.

	Temperature [°C]			
	SemiSoft	Sunlu	Geeetech	Overture
IX	255	210	240	**230**
VIII	252	207	235	227
VII	250	205	**230**	225
VI	247	202	225	222
V	245	200	220	220
IV	242	197	215	217
III	240	195	210	215
II	237	192	205	212
I	**235**	**190**	200	200

*The printer bed was preheated to 70°C for all filaments.

2.2.3. Additive Manufacturing

Three-dimensional models were designed in Creo Parametric 6.0.6.0 (PTC, Boston, Massachusetts, USA). To maintain consistency across all experiments while facilitating reproducibility, the gyroid structures were modeled in the form of discs with a diameter of 50 mm and a height of 10 mm [19]. Four Gyroid unit cell sizes (10, 8, 6, and 4 mm) were selected to represent different levels of structural coarseness. Each of these designs was further varied by applying three wall thicknesses (0.5, 0.75, and 1.0 mm) as well as three outer wall thicknesses (0.4, 0.6, and 0.8 mm), resulting in 36 unique design variants (Table A1 in the Appendix). These design variations were realized for each of the four TPU filaments under investigation, yielding a total of 144 disc specimens. The digital models were exported in STL format and subsequently processed in PrusaSlicer 2.7.4 (PRUSA Research, Prague, Czech Republic). Printing was performed on either a Prusa i3 MK3S+ (PRUSA Research) or a SOVOL SV04 printer. Prior to slicing, filament-specific extrusion parameters were adjusted in the software (see Table 2), while other settings such as 100% infill and a constant print speed were applied uniformly. Final G-code files were generated and transferred to the printers. All specimens were printed on a textured spring steel build plate, with adhesion enhanced by a thin layer of glue stick (Kores, Vienna, Austria). In addition to the disc geometries, standardized tensile test specimens (DIN EN ISO 527, Type 5A) were produced from each TPU filament at 100% infill. These samples were reserved for subsequent mechanical characterization.

2.3. Sample Characterization

 doi:10.20944/preprints202512.0888.v1

2.3.1. Microscopy

Structural evaluation of the printed specimens was carried out using a stereomicroscope (Olympus SZ61, Olympus Inc., Tokyo, Japan) equipped with an SC30 digital camera. For this purpose, discs were produced at half the height of the standard test specimens, and the printing process was deliberately paused at 50% completion in order to provide unobstructed insight into the internal gyroid geometry. In addition, selected full-height samples were bisected using razor and microtome blades. Dimensional features of the gyroid structures, including wall thickness and pore size, were quantified at multiple locations (≥5 per sample) and compared with the corresponding design specifications from the STL models. Image analysis was performed in ImageJ (FIJI version 1.53t). Scale calibration was established via Stream Motion (Olympus Inc.), which allowed measurements to be reported in metric units rather than pixel lengths. For each variant, at least 20 measurement points were collected per wall type and averaged for subsequent comparison.

2.3.2. Mechanical Properties

To assess filament-specific behavior, tensile testing was performed on dogbone specimens (DIN EN ISO 527, Type 5A) printed from four different TPU filaments (extrudr FlexSemiSoft, SUNLU TPU 95A, OVERTURE TPU 95A, GEETECH TPU 95A). Testing was carried out on a universal testing machine (LTM10, Zwick-Roell GmbH & Co. KG, Ulm, Germany), with a minimum of five replicates per filament. The mechanical response of the disc-shaped samples was examined in uniaxial compression (Zmart.Pro, Zwick-Roell GmbH & Co. KG). At least three discs per parameter set were tested. Following preload application (1 N), force–displacement data were continuously recorded at a sampling frequency of 1000 Hz while the specimens were compressed at 5 mm/min until 50% strain or a maximum load of 20 kN was reached. The software automatically terminated the test once either limit condition was met. Thickness measurements were taken with a digital caliper at five points before, immediately after, and 24 h post-compression to monitor deformation recovery. Force–displacement curves were averaged from three replicates per condition. Target force ranges for testing were derived from in vivo spinal loading data: vertebral endplates typically withstand 4000–6000 N [20], and intervertebral discs can experience up to 200–250% of body weight during daily activity or exertion [21], corresponding to ~2100 N in an 85 kg individual. To simulate possible peak loads, e.g. during trauma, a broader working window of 4000–7500 N was defined. Samples exceeding 7500 N or compressive strengths above 3.81 MPa (normalized to 50 mm disc diameter) were excluded. This threshold was chosen to reflect the larger contact area of the printed discs relative to native discs, while still aligning with previously reported physiological values (≤3.5 MPa) for intact human lumbar segments [22].

2.4. Statistics

All data are reported as mean values accompanied by their respective standard deviations. Prior to statistical testing, the distribution of the data was examined using the Shapiro–Wilk test. For comparisons between groups, a one-way ANOVA with Tukey's post hoc test was applied, considering differences significant at $p < 0.05$. Statistical processing was carried out with OriginPro 2025 SR1 (OriginLab, Northampton, USA).

3. Results

3.1. Sample Dimensions

With the temperatures optimized by the temperature towers (see Table 2), the discs with the different gyroids of varying volumes and wall thicknesses could be printed consistently. In addition, additional drying of the filaments at 55°C in the filament drying box further improved the printing result. The following Figure 2 shows examples of slices with different wall thicknesses (inner vs. outer) for the different filaments for a Gyroid volume of 8 mm³. Due to space limitations, the figures

 doi:10.20944/preprints202512.0888.v1

for SemiSoft and Overture can be found in the Appendix (Figures A1 and A2). Table 3 below compares the measured wall thicknesses with the target values from the CAD models for the various TPU filaments.

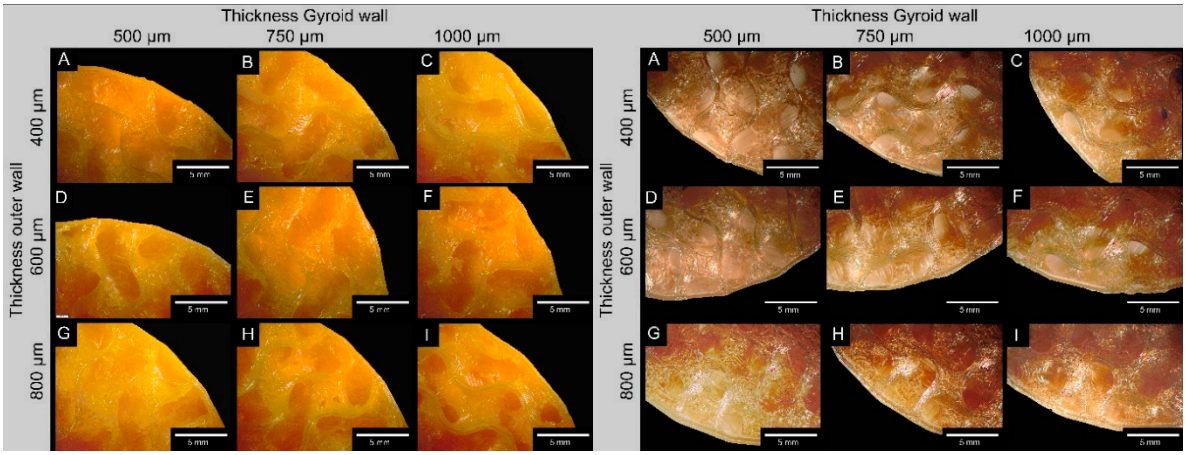

Figure 2. Representative comparison of the varying wall thicknesses of the inner and outer regions of the Gyroid structure made of SUNLU (orange) and GEEETECH TPU (brown). To facilitate accurate wall thickness measurements, 3D printing was paused at 30% to avoid potential measurement errors due to surface curvature (example shown for a 10 mm³ Gyroid volume).

Table 3. Target-performance comparison of the inner and outer walls of the Gyroid for the different filaments, as an example for the Gyroid volume of 10 mm³.

FlexSemiSoft				
Specimen	Gyroid wall (target) [mm]	Gyroid wall (measured) [mm]	Outer wall (target) [mm]	Outer wall (measured) [mm]
FS01	0.5	0.49 ± 0.03	0.4	0.40 ± 0.02
FS02	0.75	0.70 ± 0.02	0.4	0.41 ± 0.01
FS03	1.0	0.90 ± 0.03	0.4	0.42 ± 0.07
FS13	0.5	0.43 ± 0.09	0.6	0.61 ± 0.02
FS14	0.75	0.70 ± 0.07	0.6	0.63 ± 0.02
FS15	1.0	0.99 ± 0.11	0.6	0.58 ± 0.04
FS25	0.5	0.43 ± 0.04	0.8	0.75 ± 0.05
FS26	0.75	0.72 ± 0.08	0.8	0.77 ± 0.01
FS27	1.0	0.93 ± 0.05	0.8	0.74 ± 0.07
SUNLU				
SL01	0.5	0.49 ± 0.03	0.4	0.40 ± 0.02
SL02	0.75	0.70 ± 0.01	0.4	0.40 ± 0.01
SL03	1.0	0.92 ± 0.01	0.4	0.44 ± 0.07
SL13	0.5	0.51 ± 0.08	0.6	0.62 ± 0.02
SL14	0.75	0.72 ± 0.06	0.6	0.63 ± 0.02
SL15	1.0	0.99 ± 0.10	0.6	0.56 ± 0.05
SL25	0.5	0.45 ± 0.01	0.8	0.78 ± 0.05
SL26	0.75	0.74 ± 0.06	0.8	0.75 ± 0.07
SL27	1.0	0.91 ± 0.05	0.8	0.74 ± 0.01
GEEETECH				
GS01	0.5	0.49 ± 0.01	0.4	0.41 ± 0.03
GS02	0.75	0.77 ± 0.01	0.4	0.42 ± 0.02

 doi:10.20944/preprints202512.0888.v1

GS03	1.0	1.02 ± 0.06	0.4	0.39 ± 0.01
GS13	0.5	0.48 ± 0.02	0.6	0.57 ± 0.02
GS14	0.75	0.75 ± 0.01	0.6	0.62 ± 0.05
GS15	1.0	0.99 ± 0.05	0.6	0.65 ± 0.02
GS25	0.5	0.50 ± 0.03	0.8	0.82 ± 0.02
GS26	0.75	0.75 ± 0.02	0.8	0.82 ± 0.02
GS27	1.0	0.96 ± 0.04	0.8	0.81 ± 0.04
OVERTURE				
OT01	0.5	0.49 ± 0.02	0.4	0.40 ± 0.02
OT02	0.75	0.76 ± 0.01	0.4	0.41 ± 0.02
OT03	1.0	0.99 ± 0.03	0.4	0.40 ± 0.03
OT13	0.5	0.49 ± 0.05	0.6	0.61 ± 0.02
OT14	0.75	0.76 ± 0.03	0.6	0.60 ± 0.01
OT15	1.0	1.01 ± 0.04	0.6	0.60 ± 0.01
OT25	0.5	0.51 ± 0.01	0.8	0.81 ± 0.01
OT26	0.75	0.75 ± 0.01	0.8	0.81 ± 0.02
OT27	1.0	0.98 ± 0.03	0.8	0.82 ± 0.02

With the exception of minor deviations, all filaments were within the specified target range, both for the Gyroid and for the outer wall. However, there are differences between the filaments. This can be seen quite clearly in Figure 2 and Figures A1 and A2 in the Appendix in terms of print defects. In particular, Overture experienced an increased number of print defects at the lower wall thicknesses. A substantial reduction was achieved through further optimizations in printing speed and retraction. However, some drop formation and slight stringing was observed. With the other filaments, these printing errors were not as pronounced.

3.2. Mechanical Properties

3.2.1. Tensile Tests

The tensile tests were carried out in accordance with ISO EN 527 with 5A specimens. The measurements were repeated at least 5 times. Due to the nature of the machine, the samples could only be stretched up to a maximum of 250%. The measurement setup on the Zwick/Roell LTM10 is shown in the following Figure 3. The specimens were pre-tensioned to 5 N and then pulled at a rate of 1 mm/s.

 doi:10.20944/preprints202512.0888.v1

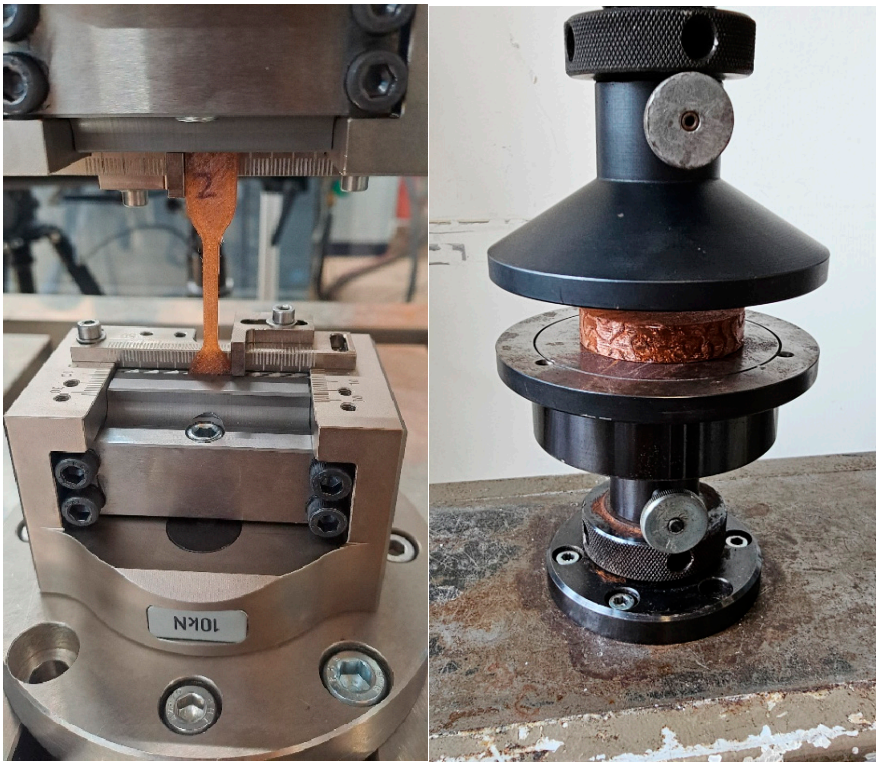

Figure 3. Mechanical Tests on OVERTUE TPU Specimen: left: Tensile test on specimens 5A (DIN ISO EN 527-2); right: compression test.

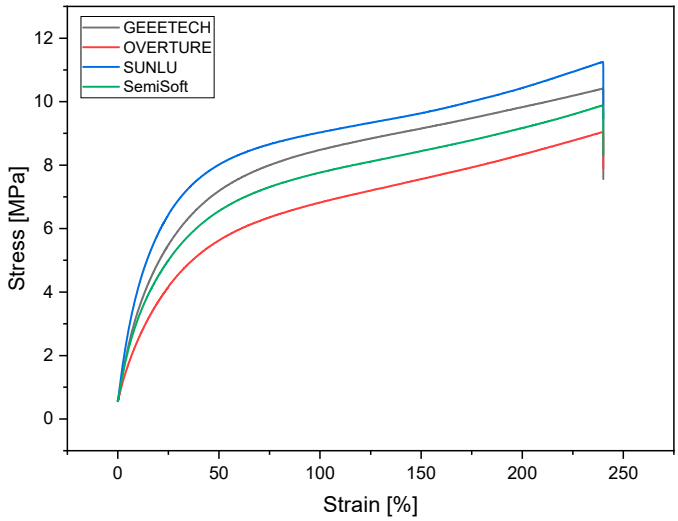

Figure 4. Stress-Strain Curves for the different TPU filaments.

The stress-strain curves of the four distinct TPU filaments (GEEETECH, OVERTURE, SUNLU, and SemiSoft) manifest conspicuous viscoelastic behavior, accompanied by elevated ductility (Figure 4). It has been demonstrated that all samples achieve maximum elongations of 250% without brittle fracture, depending on the testing machine. The curves are characterized by an initially steep rise in the elastic range, followed by plastic-viscous flow with moderate stress hardening. GEEETECH and SUNLU demonstrated the highest tensile strengths, at 10.6 ± 0.2 MPa and 10.9 ± 0.15 MPa, respectively, and exhibited substantial hardening with increasing elongation. These materials are well suited for functional applications that require both strength and elastic recovery. In contrast, OVERTURE exhibited the lowest overall load values (9.1 ± 0.05 MPa) and reduced stiffness in the initial range, suggesting a softer material behavior. SemiSoft exhibits a balanced profile between

 doi:10.20944/preprints202512.0888.v1

stiffness and elongation capacity, with a reading of 10.0 ± 0.07 MPa. The tensile modulus of SUNLU TPU was the highest of all filaments tested at 29.3 ± 2.2 MPa. The tensile modulus results of Sunlu, Geeetech and SemiSoft were not significantly different. A similar result was found for the compressive strength of the four filaments. Figure 5 and Table 4 summarize the results for tensile modulus and compressive strength.

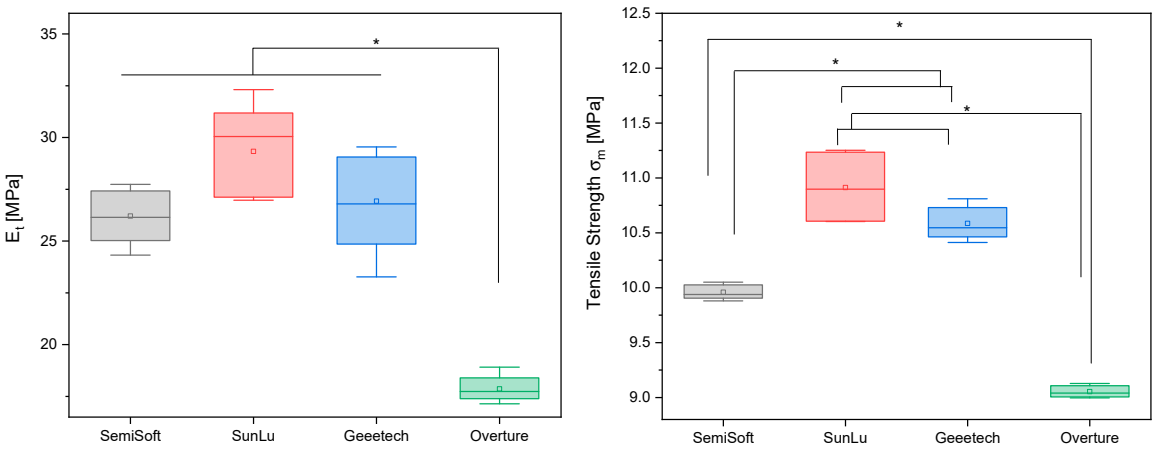

Figure 5. Tensile modulus and tensile strength of the four analyzed filaments; $p<0.05$ (*).

There is no significant difference between the filaments of SemiSoft, SUNLU, and GEEETECH in terms of tensile modulus ($p > 0.05$). However, OVERTURE´s filament differs significantly from the other three manufacturers in terms of tensile modulus, with $p<0.0001$. The filaments of SUNLU and GEEETECH do not differ significantly from each other in terms of tensile strength, with $p = 0.83$. But the filament of SemiSoft differs significantly from SUNLU ($p < 0.01$), GEEETECH ($p < 0.01$), and OVERTURE ($p < 0.001$) in terms of tensile strength. The same applies to the significant differences in tensile strength between OVERTURE and SUNLU ($p < 0.001$) and between OVERTURE and GEEETECH ($p < 0.001$).

Table 4. Summary of the results of the tensile test according to DIN EN ISO 527-1 with a maximum strain of 250% (machine-related); n=5.

SemiSoft	**E_t [MPa]**	**σ_x [MPa]**	**σ_m [MPa]**	**ε_m [%]**
Mean	26.2	3.2	10.0	240.6
Min	24.3	3.1	9.9	239.7
Max	27.7	3.2	10.1	241.3
SD	1.3	0.03	0.1	0.6
SUNLU	**E_t [MPa]**	**σ_x [MPa]**	**σ_m [MPa]**	**ε_m [%]**
Mean	29.3	3.9	10.9	240.0
Min	27.0	3.6	10.0	239.6
Max	32.3	4.1	11.3	240.8
SD	2.2	0.2	0.2	0.4
GEEETECH	**E_t [MPa]**	**σ_x [MPa]**	**σ_m [MPa]**	**ε_m [%]**
Mean	26.9	3.5	10.6	240.7
Min	23.3	3.4	10.4	239.8
Max	29.6	3.6	10.8	241.6
SD	2.4	0.1	0.2	0.7

 doi:10.20944/preprints202512.0888.v1

OVERTURE	E_t [MPa]	σ_X [MPa]	σ_m [MPa]	ε_m [%]
Mean	17.9	2.5	9.1	239
Min	17.1	2.4	9.0	237.5
Max	18.9	2.5	9.1	239.9
SD	0.6	0.02	0.1	0.9

3.2.2. Compression Tests

3.2.2.1. SemiSoft

As can be seen in Figure 6, only two samples are within the specified range. These are samples FS23 with F_{max} of 6918 ± 66 N and compressive strength of 3.52 ± 0.03 MPa) and FS33 with F_{max} of 4171 ± 38 N and compressive strength of 2.13 ± 0.02 MPa.

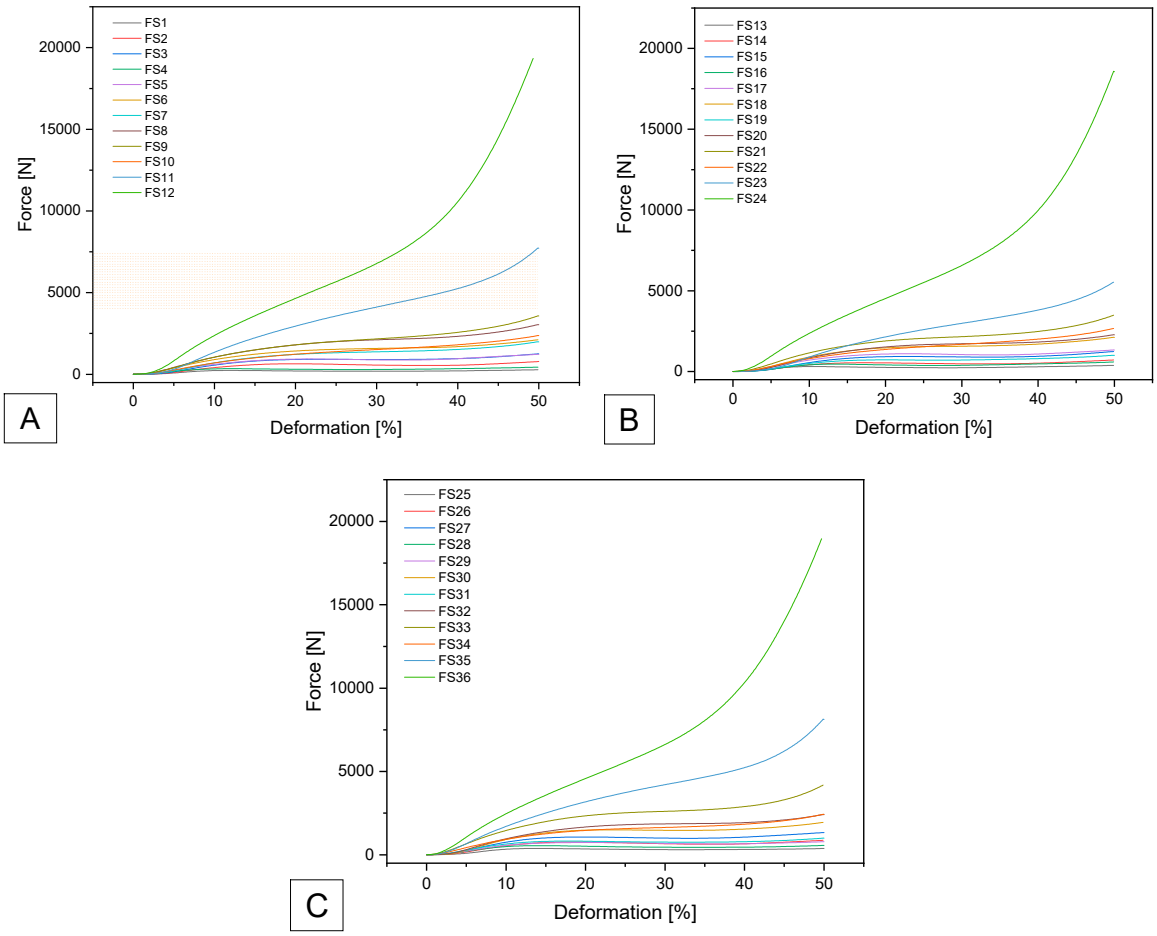

Figure 6. Force-deformation curves for the additively manufactured Gyroid structures with A: 0.4 mm; B: 0.6 mm and C: 0.8 mm outer wall thickness using SemiSoft Filament.

3.2.2.2. SUNLU

For SUNLU filament, three samples: SL11; SL21 and SL33 were within the specified range. SL11 achieved F_{max} of 6607 ± 267 N and compressive strength of 3.4 ± 0.16 MPa; SL21 achieved F_{max} of 5718 ± 222 N and 2.9 ± 0.11 MPa and SL33 achieved F_{max} of 6123 ± 207 N and compressive strength of 3.1 ± 0.08 MPa (see Figure 7).

 doi:10.20944/preprints202512.0888.v1

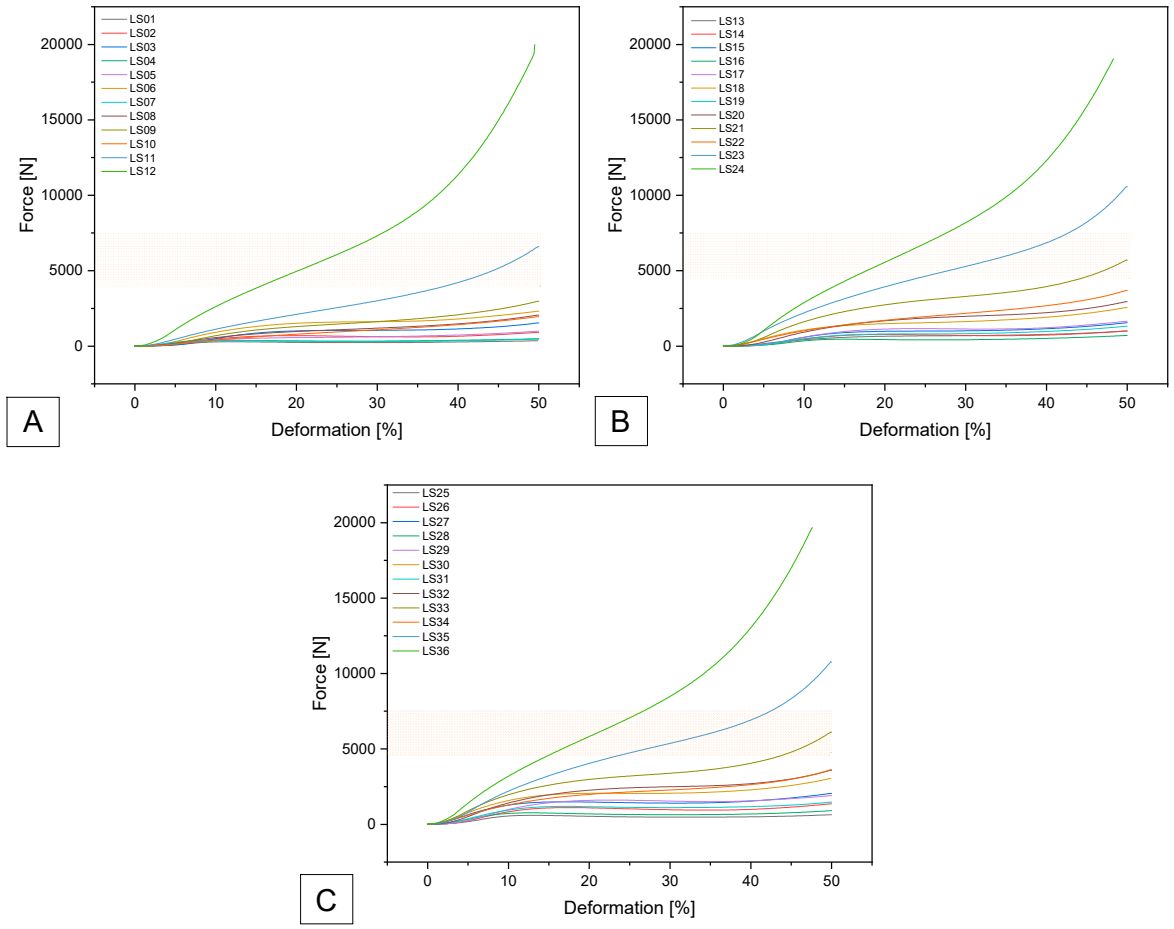

Figure 7. Force-deformation curves for the additively manufactured Gyroid structures with A: 0.4 mm; B: 0.6 mm and C: 0.8 mm outer wall thickness using SUNLU TPU Filament.

3.2.2.3. GEEETECH

Samples GS07, GS21 and GS33 were within the specification. GS07 had a maximum force of 5533 ± 38 N and a compressive strength of 2.81 ± 0.06 MPa. GS 21 was in a similar range of the maximum tolerated force with 5935 ± 221 N and a compressive strength of 3.02 ± 0.09 MPa. GS33 was also in the same range with 5542 ± 190 N and 2.82 ± 0.08 MPa (see Figure 8).

 doi:10.20944/preprints202512.0888.v1

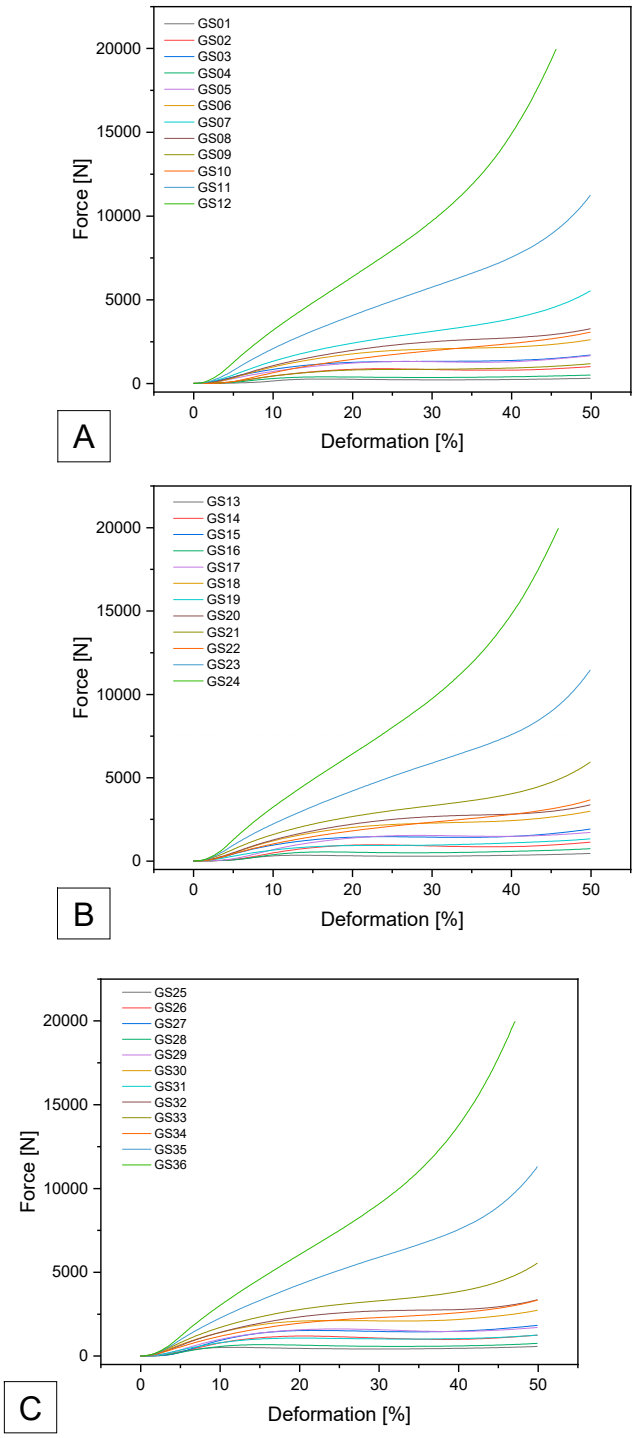

Figure 8. Force-deformation curves for the additively manufactured Gyroid structures with A: 0.4 mm; B: 0.6 mm and C: 0.8 mm outer wall thickness using GEEETECH TPU Filament.

3.2.2.4. OVERTURE

The samples OT09, OT21 and OT33 met the specified requirements. OT09 had a maximum load of 4585 ± 117 N and a compressive strength of 2.29 ± 0.06 MPa. OT21 showed comparable values with a maximum load of 5171 ± 45 N and a compressive strength of 2.55 ± 0.02 MPa. Similarly, OT33 achieved 4922 ± 69 N and 2.38 ± 0.03 MPa (see Figure 9).

 doi:10.20944/preprints202512.0888.v1

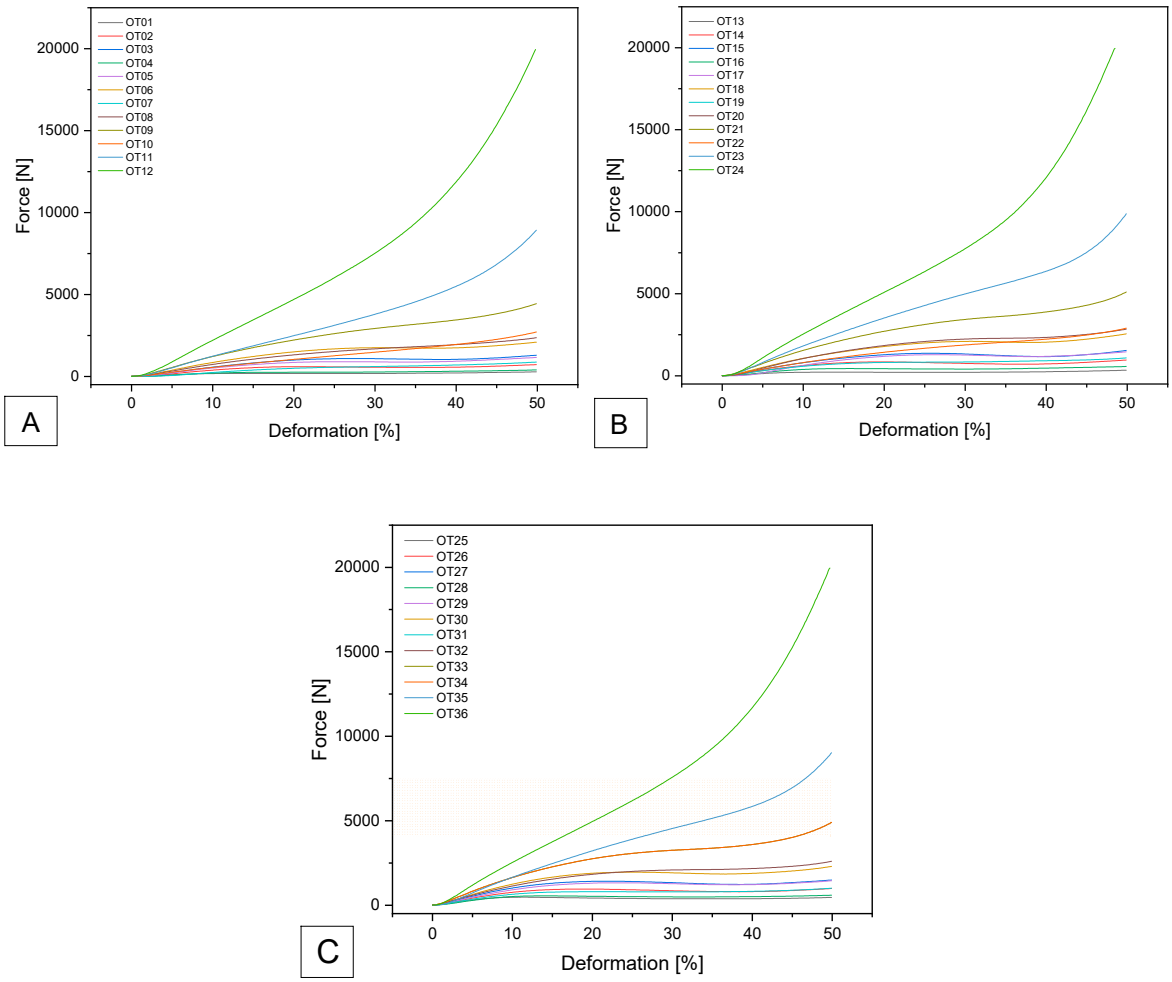

Figure 9. Force-deformation curves for the additively manufactured Gyroid structures with A: 0.4 mm; B: 0.6 mm and C: 0.8 mm outer wall thickness using OVERTURE TPU Filament.

The actual values achieved in the maximum tolerated force for the tested samples are summarized in Table 5. The dimensions of all samples that were within the specification were summarized in the following Table 6.

Table 5. Overview of the samples from the different filaments and their outer wall thicknesses that were in the target range of 4000-7500N with their F_{max} and compressive strength (n=3).

Extrudr FlexSemiSoft								
0.4 mm			**0.6 mm**			**0.8 mm**		
Sample	**Fmax [N]**	**σ_D [MPa]**	**Sample**	**Fmax [N]**	**σ_D [MPa]**	**Sample**	**Fmax [N]**	**σ_D [MPa]**
-	-	-	FS23	6918 ± 66	3.52 ± 0.03	FS33	4171 ± 38	2.13 ± 0.02
SUNLU TPU								
0.4 mm			**0.6 mm**			**0.8 mm**		
Sample	**Fmax [N]**	**σ_D [MPa]**	**Sample**	**Fmax [N]**	**σ_D [MPa]**	**Sample**	**Fmax [N]**	**σ_D [MPa]**
SL11	6607 ± 267	3.4 ± 0.16	SL21	5718 ± 222	2.9 ± 0.11	SL33	6123 ± 207	3.1 ± 0.08
GEEETECH TPU								
0.4 mm			**0.6 mm**			**0.8 mm**		

 doi:10.20944/preprints202512.0888.v1

Sample	Fmax [N]	σ_D [MPa]	Sample	Fmax [N]	σ_D [MPa]	Sample	Fmax [N]	σ_D [MPa]
GS07	5533 ± 38	2.81 ± 0.06	GS21	5935 ± 221	3.02 ± 0.09	GS33	5542 ± 190	2.82 ± 0.08
OVERTURE TPU								
0.4 mm			**0.6 mm**			**0.8 mm**		
Sample	**Fmax [N]**	**σ_D [MPa]**	**Sample**	**Fmax [N]**	**σ_D [MPa]**	**Sample**	**Fmax [N]**	**σ_D [MPa]**
OT09	4585 ± 117	2.29 ± 0.06	OT21	5171 ± 45	2.55 ± 0.02	OT33	4922 ± 69	2.38 ± 0.03

Table 6. Summary of sample dimensions within the target range of 4000-7500N.

Sample	Gyroid size [mm]	Gyroid Wall [mm]	Outer Wall [mm]
Extrudr FlexSemiSoft			
FS23	4	0.75	0.6
FS33	6	1.0	0.8
SUNLU TPU			
SL11	4	0.75	0.4
SL21	6	1.0	0.6
SL33	6	1.0	0.8
GEEETECH TPU			
GS07	6	0.5	0.4
GS21	6	1.0	0.6
GS33	6	1.0	0.8
OVERTURE TPU			
OT09	6	1.0	0.4
OT21	6	1.0	0.6
OT33	6	1.0	0.8

3.2.3. Sample Height

Sample height was measured using a digital caliper before, immediately after, and 24 hours after the mechanical tests. It was found that after compression to 50% of the height, the specimens required a period of time to return to their original height. After 24 hours, all specimens had returned to their original height. The following Figure 10 summarize the specimen height distribution for the specimens in the 4000-7500N target range.

 doi:10.20944/preprints202512.0888.v1

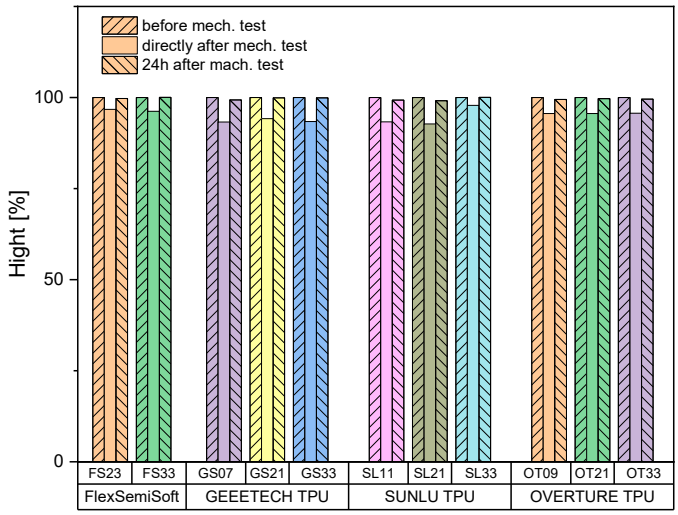

Figure 10. Sample heights before, immediately after, and 24 hours after the mechanical test for all samples which were in the target range of 4000-7500 N.

4. Discussion

Although all of the filaments tested in this work were specified by the manufacturer to have a Shore hardness of 85A or 95A, the filaments differed significantly in their properties in both tensile and compression tests, as well as in their 3D printability. The TPU filaments tested in this work were significantly softer than the FlexMed and FlexHard filaments we had previously tested [19] with a Shore hardness of 95A as specified by the manufacturer. Nevertheless, Sunlu and Geeetech exhibited analogous values for tensile strength and tensile modulus. SemiSoft exhibited a similar trend but demonstrated a substantial disparity in tensile strength. The TPU from Overture exhibited marked differences from the other three filaments in all cases. The tensile strength of SemiSoft was only 1/5 that of FlexHard and 1/3 that of FlexMed from our previous work [19]. A parallel situation was observed for the SUNLU and GEEETECH TPU filaments. In fact, the OVERTURE filament was only 1/10 the strength of FlexHard and 1/6 the strength of FlexMed. Shin et al. [23] described a similarly strong TPU filament with 19.9 MPa, which they also 3D printed using FDM at 180~220°C. Harynska et al. [24] also printed their TPU for medical applications using FDM, but at 200°C, achieving a comparable tensile strength of 26 ± 2 MPa. However, Shin et al [25] printed their TPU as pellets, not filaments, at 190°C and achieved tensile strengths between 7.42 and 26.93 MPa, depending on the composition. By blending TPU with ABS, Soltanmohammadi et al. [26] achieved compressive strengths in over 150 MPa.

Bayati et al [27] argue that in extrusion-based 3D printing, the orifice through which the material is extruded is circular, resulting in cylindrical print paths. When these paths are layered and joined together to form the final object, gaps or spaces are often created between the layers [28]. This is illustrated in Figure 4, which shows a cross-section of a printed part. The size of these spaces, also known as voids, depends on the print quality. Optimal printing parameters and high printability reduce these voids, resulting in a more uniform microstructure of the printed part [29]. Improved overlap, material flow, and wettability minimize voids, thereby improving the mechanical properties of the part [30]. However, the presence of voids can contribute to damage in printed samples. Stresses can develop at the layer interfaces, which can promote crack growth or delamination [31]. These defects, combined with external stresses or environmental factors, can compromise the structural integrity of the printed object and lead to failure or reduced performance over time. This is exactly what we observed with the flexible TPU filaments. Because the Prusa MK3S+ extruder had difficulty with the TPU filament, there was some stringing and drooling on the prints, but they were otherwise flawless.

 doi:10.20944/preprints202512.0888.v1

Regarding the recovery of the tested discs, we were able to determine, analogous to Feki et al. [32] or Goode and Teodore [33], that our discs behave like intervertebral discs and return to their original thickness overnight. How is this effect achieved? The osmotic pressure of the nucleus pulposus counteracts this stress; however, it is often exceeded during physical activity, resulting in the displacement of water from the disc [34,35].This process leads to a reduction in disc height and volume [36–38]. During overnight rest, the decrease in external loading allows the osmotic pressure of the nucleus to reabsorb water, facilitating rehydration of the disc [39–41].While some research suggests that loss of disc height is due to radial expansion of the annulus fibrosus [42,43]. Botsford et al [38] argue in their study of diurnal disc changes that such radial bulging is minimal during typical daily activities. They claim that the main factor contributing to the reduction in disc height is the loss of fluid from the disc itself. It is noteworthy that a healthy intervertebral disc can fully recover its original pressure, height, and volume despite being loaded twice as long during the day as during the resting phase at night.

5. Conclusion

In this study, a comprehensive test matrix comprising four different Gyroid sizes, each combined with three wall thicknesses and three outer wall configurations, resulting in 36 distinct specimens per filament, was evaluated across four TPU filaments. By applying an optimized drying protocol at 55 °C prior to and during the printing process, filaments that had been unprintable in a previous study [19] were successfully processed, with substantial reductions in printing errors such as stringing and droplet formation. The TPU filaments with Shore hardness 95A displayed increased flexibility compared to previously reported 95A materials, with 2–3 Gyroid structures per filament achieving peak loads within the target range of 4000–7500 N. These findings indicate that structural variation in Gyroid geometry and wall design can significantly influence the mechanical performance of printed samples. Compared with rigid UHMWPE and titanium implants, the additively manufactured TPU Gyroid structures produced via FDM demonstrate promising shock-absorbing capabilities, reinforcing their potential as intervertebral disc substitutes. Clinically, these results emphasize the importance of tailoring internal architecture to optimize biomechanical properties. Future work should extend to intervertebral disc–shaped specimens with and without outer walls, under both static and dynamic loading conditions, while also accounting for the natural three-dimensional curvature of discs.

Author Contributions: LH, JM and MS performed the preparation procedure, mechanical testing, data analysis, and statistics. LH and MS drafted the manuscript. DV, BR and HS participated in the design and coordination of the study. MS and BR conceived the study. MS supervised the study. BR and HS provided resources. All authors read and approved the final manuscript.

Funding: The author(s) declare that financial support was received for the research, authorship, and/or publication of this article. The processing fee for the article was financed by the Ministry of Science, Research and the Arts Baden-Württemberg and the University of Freiburg as part of the Open Access Publishing funding program.

Institutional Review Board Statement: Not applicable.

Informed Consent Statement: Not applicable.

Data Availability Statement: The data presented in this study are available on request from the corresponding author.

Acknowledgments: The authors would like to thank Sunil Shetty, a native speaker, for spell-checking and grammar correction.

Conflicts of Interest: The authors declare no conflicts of interest.

 doi:10.20944/preprints202512.0888.v1

List of abbreviations

ASD	adjacent segment degeneration
CAD	computer aided design
FDM	fused deposition modelling
FS	Flex Semisoft Filament Sample
G-code	geometry code
GS	Geeetech TPU Filament Sample
OT	Overture TPU Filament Sample
ROM	range of motion
SL	Sunlu TPU Filament Sample
STL	stereo lithography file
TPU	thermoplastic polyurethane

Not listed here are SI abbreviations.

Appendix A

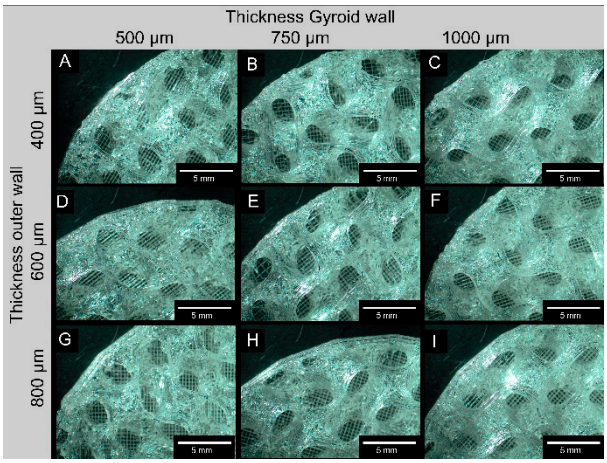

Figure A1. Representative comparison of the varying wall thicknesses of the inner and outer regions of the Gyroid structure made of SemiSoft. To facilitate accurate wall thickness measurements, 3D printing was paused at 30% to avoid potential measurement errors due to surface curvature (example shown for a 8 mm^3 Gyroid volume).

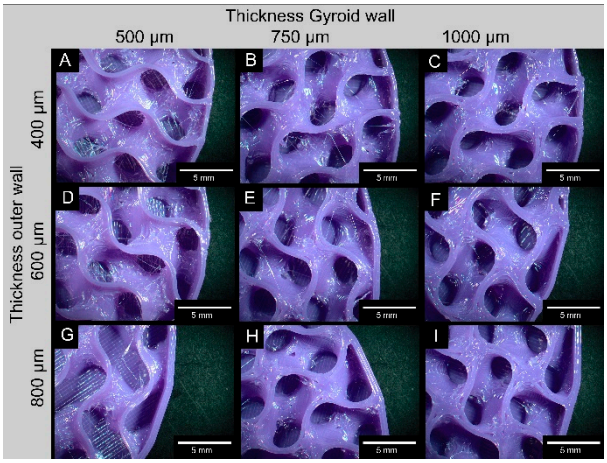

Figure A2. Representative comparison of the varying wall thicknesses of the inner and outer regions of the Gyroid structure made of OVERTURE TPU. To facilitate accurate wall thickness measurements, 3D printing was

 doi:10.20944/preprints202512.0888.v1

paused at 30% to avoid potential measurement errors due to surface curvature (example shown for a 8 mm³ Gyroid volume).

Table A1. Gyroid Dimensions for additive manufacturing for each Filament.

Sample	Gyroid Dimensions		
	Volume [mm³]	Wall thickness Gyroid [mm]	Wall thickness outer wall [mm]
#01	10	0.5	0.4
#02	10	0.75	0.4
#03	10	1.0	0.4
#04	8	0.5	0.4
#05	8	0.75	0.4
#06	8	1.0	0.4
#07	6	0.5	0.4
#08	6	0.75	0.4
#09	6	1.0	0.4
#10	4	0.5	0.4
#11	4	0.75	0.4
#12	4	1.0	0.4
#13	10	0.5	0.6
#14	10	0.75	0.6
#15	10	1.0	0.6
#16	8	0.5	0.6
#17	8	0.75	0.6
#18	8	1.0	0.6
#19	6	0.5	0.6
#20	6	0.75	0.6
#21	6	1.0	0.6
#22	4	0.5	0.6
#23	4	0.75	0.6
#24	4	1.0	0.6
#25	10	0.5	0.8
#26	10	0.75	0.8
#27	10	1.0	0.8
#28	8	0.5	0.8
#29	8	0.75	0.8
#30	8	1.0	0.8
#31	6	0.5	0.8
#32	6	0.75	0.8
#33	6	1.0	0.8
#34	4	0.5	0.8
#35	4	0.75	0.8
#36	4	1.0	0.8

References

1. Abudouaini, H., T. Wu, Y. Meng, B. Wang, et al., *Mechanical properties of an elastically deformable cervical spine implant.* Journal of Orthopaedic Surgery and Research, **2023**. 18(1): p. 605 DOI: https://doi.org/10.1186/s13018-023-04042-7.

2. Goedmakers, C.M.W., F. de Vries, L. Bosscher, W.C. Peul, et al., *Long-term results of the NECK trial—implanting a disc prosthesis after cervical anterior discectomy cannot prevent adjacent segment disease: five-year clinical follow-up of a double-blinded randomised controlled trial.* The Spine Journal, **2023**. 23(3): p. 350–360 DOI: https://doi.org/10.1016/j.spinee.2022.11.006.
3. Abi-Hanna, D., J. Kerferd, K. Phan, P. Rao, et al., *Lumbar Disk Arthroplasty for Degenerative Disk Disease: Literature Review.* World Neurosurgery, **2018**. 109: p. 188–196 DOI: https://doi.org/10.1016/j.wneu.2017.09.153.
4. Li, J., P. OuYang, X. He, X. Wei, et al., *Cervical non-fusion using biomimetic artificial disc and vertebra complex: technical innovation and biomechanics analysis.* Journal of Orthopaedic Surgery and Research, **2022**. 17(1): p. 122 DOI: https://doi.org/10.1186/s13018-022-03012-9.
5. Cui, X.-D., H.-T. Li, W. Zhang, L.-L. Zhang, et al., *Mid- to long-term results of total disc replacement for lumbar degenerative disc disease: a systematic review.* Journal of Orthopaedic Surgery and Research, **2018**. 13(1): p. 326 DOI: https://doi.org/10.1186/s13018-018-1032-6.
6. Gornet, M.F., T.H. Lanman, J.K. Burkus, S.D. Hodges, et al., *Cervical disc arthroplasty with the Prestige LP disc versus anterior cervical discectomy and fusion, at 2 levels: results of a prospective, multicenter randomized controlled clinical trial at 24 months.* J Neurosurg Spine, **2017**. 26(6): p. 653–667 DOI: https://doi.org/10.3171/2016.10.Spine16264.
7. Shen, Y.-W., Y. Yang, H. Liu, X. Rong, et al., *Effects of endplate coverage and intervertebral height change on heterotopic ossification following cervical disc replacement.* Journal of Orthopaedic Surgery and Research, **2021**. 16(1): p. 693 DOI: https://doi.org/10.1186/s13018-021-02840-5.
8. Pham, M., K. Phan, I. Teng, and R.J. Mobbs, *Comparative Study Between M6-C and Mobi-C Cervical Artificial Disc Replacement: Biomechanical Outcomes and Comparison with Normative Data.* Orthop Surg, **2018**. 10(2): p. 84–88 DOI: https://doi.org/10.1111/os.12376.
9. Feng, H., X. Fang, D. Huang, C. Yu, et al., *Quantitative morphometric study of the subaxial cervical vertebrae end plate.* The Spine Journal, **2017**. 17(2): p. 269–276 DOI: https://doi.org/10.1016/j.spinee.2016.09.019.
10. Patwardhan, A.G. and R.M. Havey, *Prosthesis design influences segmental contribution to total cervical motion after cervical disc arthroplasty.* European Spine Journal, **2020**. 29(11): p. 2713–2721 DOI: https://doi.org/10.1007/s00586-019-06064-4.
11. destatis, *Fallpauschalenbezogene Krankenhausstatistik (DRG-Statistik) Operationen und Prozeduren der vollstationären Patientinnen und Patienten in Krankenhäusern (4-Steller) für 2021*, G.F.S. Office, Editor. 2022: Wiesbaden.
12. Cloyd, J.M., N.R. Malhotra, L. Weng, W. Chen, et al., *Material properties in unconfined compression of human nucleus pulposus, injectable hyaluronic acid-based hydrogels and tissue engineering scaffolds.* Eur Spine J, **2007**. 16(11): p. 1892–8 DOI: https://doi.org/10.1007/s00586-007-0443-6.
13. Warburton, A., S.J. Girdler, C.M. Mikhail, A. Ahn, et al., *Biomaterials in Spinal Implants: A Review.* Neurospine, **2020**. 17(1): p. 101–110 DOI: https://doi.org/10.14245/ns.1938296.148.
14. Serra, T., C. Capelli, R. Toumpaniari, I.R. Orriss, et al., *Design and fabrication of 3D-printed anatomically shaped lumbar cage for intervertebral disc (IVD) degeneration treatment.* Biofabrication, **2016**. 8(3): p. 035001 DOI: https://doi.org/10.1088/1758-5090/8/3/035001.
15. Marshall, S.L., T.D. Jacobsen, E. Emsbo, A. Murali, et al., *Three-Dimensional-Printed Flexible Scaffolds Have Tunable Biomimetic Mechanical Properties for Intervertebral Disc Tissue Engineering.* ACS Biomaterials Science & Engineering, **2021**. 7(12): p. 5836–5849 DOI: https://doi.org/10.1021/acsbiomaterials.1c01326.
16. Fidai, A.B., B. Kim, M. Lintz, S. Kirnaz, et al., *Flexible support material maintains disc height and supports the formation of hydrated tissue engineered intervertebral discs in vivo.* **2024**. 7(3): p. e1363 DOI: https://doi.org/10.1002/jsp2.1363.
17. Obaid, M.N., N.A. Berto, and S.H. Radhi, *Preparation and characterization of UHMWPE reinforced with polyester fibers for artificial cervical disc replacement (ACDR).* J Biomater Sci Polym Ed, **2023**. 34(12): p. 1758–1769 DOI: 10.1080/09205063.2023.2182576.
18. Xiao, J. and Y. Gao, *The manufacture of 3D printing of medical grade TPU.* Progress in Additive Manufacturing, **2017**. 2(3): p. 117–123 DOI: https://doi.org/10.1007/s40964-017-0023-1.

19. Gross, V., S. Zankovic, B. Rolauffs, D. Velten, et al., *On the suitability of additively manufactured gyroid structures and their potential use as intervertebral disk replacement - a feasibility study.* Frontiers in Bioengineering and Biotechnology, **2024**. 12 DOI: https://doi.org/10.3389/fbioe.2024.1432587.
20. Wang, B.H. and G. Campbell, *Formulations of polyvinyl alcohol cryogel that mimic the biomechanical properties of soft tissues in the natural lumbar intervertebral disc.* Spine (Phila Pa 1976), **2009**. 34(25): p. 2745–53 DOI: https://doi.org/10.1097/BRS.0b013e3181b4abf5.
21. Rohlmann, A., H.-J. Wilke, H. Mellerowicz, F. Graichen, et al., *Loads on the spine in sports.* German Journal of Sports Medicine, **2001**. 52(4): p. 118–123.
22. Wilke, H.J., P. Neef, M. Caimi, T. Hoogland, et al., *New in vivo measurements of pressures in the intervertebral disc in daily life.* Spine (Phila Pa 1976), **1999**. 24(8): p. 755–62 DOI: https://doi.org/10.1097/00007632-199904150-00005.
23. Shin, E.J., Y.S. Jung, H.Y. Choi, and S. Lee, *Synthesis and fabrication of biobased thermoplastic polyurethane filament for FDM 3D printing.* Journal of Applied Polymer Science, **2022**. 139(40): p. e52959 DOI: https://doi.org/10.1002/app.52959.
24. Haryńska, A., I. Gubanska, J. Kucinska-Lipka, and H. Janik, *Fabrication and Characterization of Flexible Medical-Grade TPU Filament for Fused Deposition Modeling 3DP Technology.* Polymers, **2018**. 10(12): p. 1304 DOI: https://doi.org/10.3390/polym10121304.
25. Shin, E.J., Y. Park, Y.S. Jung, H.Y. Choi, et al., *Fabrication and characteristics of flexible thermoplastic polyurethane filament for fused deposition modeling three-dimensional printing.* Polymer Engineering and Science, **2022**. 62(9): p. 2947–2957 DOI: https://doi.org/10.1002/pen.26075.
26. Soltanmohammadi, K., D. Rahmatabadi, M. Aberoumand, E. Soleyman, et al., *Effects of TPU on the mechanical properties, fracture toughness, morphology, and thermal analysis of 3D-printed ABS-TPU blends by FDM.* Vinyl Additive Technology, **2024**. 30(4): p. 958–968 DOI: https://doi.org/10.1002/vnl.22097.
27. Bayati, A., M. Ahmadi, D. Rahmatabadi, M. Khodaei, et al., *3D printed elastomers with superior stretchability and mechanical integrity by parametric optimization of extrusion process using Taguchi Method.* Materials Research Express, **2025**. 12(1): p. 015301 DOI: https://doi.org/10.1088/2053-1591/ada1a6.
28. Syrlybayev, D., B. Zharylkassyn, A. Seisekulova, M. Akhmetov, et al., *Optimisation of Strength Properties of FDM Printed Parts—A Critical Review.* Polymers, **2021**. 13(10): p. 1587.
29. Gupta, C., P. MB, N.K. Shet, A.K. Ghosh, et al., *Microstructure and mechanical performance examination of 3D printed acrylonitrile butadiene styrene thermoplastic parts.* **2020**. 60(11): p. 2770–2781 DOI: https://doi.org/10.1002/pen.25507.
30. Rahmatabadi, D., A. Bayati, M. Khajepour, K. Mirasadi, et al., *Poly(ethylene terephthalate) glycol/carbon black composites for 4D printing.* Materials Chemistry and Physics, **2024**. 325: p. 129737 DOI: https://doi.org/10.1016/j.matchemphys.2024.129737.
31. Rahmatabadi, D., M. Khajepour, A. Bayati, K. Mirasadi, et al., *Advancing sustainable shape memory polymers through 4D printing of polylactic acid-polybutylene adipate terephthalate blends.* European Polymer Journal, **2024**. 216: p. 113289 DOI: https://doi.org/10.1016/j.eurpolymj.2024.113289.
32. Feki, F., F. Zaïri, A. Tamoud, M. Moulart, et al., *Understanding the Recovery of the Intervertebral Disc: A Comprehensive Review of In Vivo and In Vitro Studies.* Journal of Bionic Engineering, **2024**. 21(4): p. 1919–1948 DOI: https://doi.org/10.1007/s42235-024-00542-2.
33. Goode, J.D. and B.M. Theodore, *Voluntary and Diurnal Variation in Height and Associated Surface Contour Changes in Spinal Curves.* Engineering in Medicine, **1983**. 12(2): p. 99–101 DOI: https://doi.org/10.1243/EMED_JOUR_1983_012_026_02.
34. Urban, J.P.G. and A. Maroudas, *Swelling of the Intervertebral Disc in Vitro.* Connective Tissue Research, **1981**. 9(1): p. 1–10 DOI: https://doi.org/10.3109/03008208109160234.
35. Urban, J.P. and J.F. McMullin, *Swelling pressure of the lumbar intervertebral discs: influence of age, spinal level, composition, and degeneration.* Spine (Phila Pa 1976), **1988**. 13(2): p. 179–87 DOI: https://doi.org/10.1097/00007632-198802000-00009.
36. Reilly, T., A. Tyrrell, and J.D. Troup, *Circadian variation in human stature.* Chronobiol Int, **1984**. 1(2): p. 121–6 DOI: https://doi.org/10.3109/07420528409059129.

 doi:10.20944/preprints202512.0888.v1

37. Tyrrell, A.R., T. Reilly, and J.D. Troup, *Circadian variation in stature and the effects of spinal loading.* Spine (Phila Pa 1976), **1985**. 10(2): p. 161–4 DOI: https://doi.org/10.1097/00007632-198503000-00011.
38. Botsford, D.J., S.I. Esses, and D.J. Ogilvie-Harris, *In vivo diurnal variation in intervertebral disc volume and morphology.* Spine (Phila Pa 1976), **1994**. 19(8): p. 935–40 DOI: https://doi.org/10.1097/00007632-199404150-00012.
39. Adams, M.A., P. Dolan, W.C. Hutton, and R.W. Porter, *Diurnal changes in spinal mechanics and their clinical significance.* J Bone Joint Surg Br, **1990**. 72(2): p. 266–70 DOI: https://doi.org/10.1302/0301-620x.72b2.2138156.
40. McMillan, D.W., G. Garbutt, and M.A. Adams, *Effect of sustained loading on the water content of intervertebral discs: implications for disc metabolism.* Ann Rheum Dis, **1996**. 55(12): p. 880–7 DOI: https://doi.org/10.1136/ard.55.12.880.
41. Malko, J.A., W.C. Hutton, and W.A. Fajman, *An in vivo MRI study of the changes in volume (and fluid content) of the lumbar intervertebral disc after overnight bed rest and during an 8-hour walking protocol.* J Spinal Disord Tech, **2002**. 15(2): p. 157–63 DOI: https://doi.org/10.1097/00024720-200204000-00012.
42. Adams, M.A. and W.C. Hutton, *The effect of posture on the fluid content of lumbar intervertebral discs.* Spine (Phila Pa 1976), **1983**. 8(6): p. 665–71 DOI: https://doi.org/10.1097/00007632-198309000-00013.
43. Adams, M.A. and P. Dolan, *Recent advances in lumbar spinal mechanics and their clinical significance.* Clin Biomech (Bristol), **1995**. 10(1): p. 3–19 DOI: https://doi.org/10.1016/0268-0033(95)90432-9.